AIP | Review of Scientific Instruments

Modeling thin-film piezoelectric polymer ultrasonic sensors

M. G. González, P. A. Sorichetti, and G. D. Santiago

Citation: Review of Scientific Instruments **85**, 115005 (2014); doi: 10.1063/1.4901966
View online: http://dx.doi.org/10.1063/1.4901966
View Table of Contents: http://scitation.aip.org/content/aip/journal/rsi/85/11?ver=pdfcov
Published by the AIP Publishing

Modeling thin-film piezoelectric polymer ultrasonic sensors

M. G. González,[1,2,a)] P. A. Sorichetti,[3] and G. D. Santiago[1]

[1]*Grupo de Láser, Óptica de Materiales y Aplicaciones Electromagnéticas (GLOMAE), Departamento de Física, Facultad de Ingeniería, Universidad de Buenos Aires, Paseo Colón 850, C1063ACV Buenos Aires, Argentina*
[2]*Consejo Nacional de Investigaciones Científicas y Técnicas (CONICET), Buenos Aires, Argentina*
[3]*Grupo de Sistemas Dispersos-Laboratorio de Sistemas Líquidos (GSD-LSL), Departamento de Física, Facultad de Ingeniería, Universidad de Buenos Aires, Paseo Colón 850, C1063ACV Buenos Aires, Argentina*

(Received 4 September 2014; accepted 5 November 2014; published online 20 November 2014)

This paper presents a model suitable to design and characterize broadband thin film sensors based on piezoelectric polymers. The aim is to describe adequately the sensor behavior, with a reasonable number of parameters and based on well-known physical equations. The mechanical variables are described by an acoustic transmission line. The electrical behavior is described by the quasi-static approximation, given the large difference between the velocities of propagation of the electrical and mechanical disturbances. The line parameters include the effects of the elastic and electrical properties of the material. The model was validated with measurements of a poly(vinylidene flouride) sensor designed for short-pulse detection. The model variables were calculated from the properties of the polymer at frequencies between 100 Hz and 30 MHz and at temperatures between 283 K and 313 K, a relevant range for applications in biology and medicine. The simulations agree very well with the experimental data, predicting satisfactorily the influence of temperature and the dielectric properties of the polymer on the behavior of the sensor. Conversely, the model allowed the calculation of the material dielectric properties from the measured response of the sensor, with good agreement with the published values. © *2014 AIP Publishing LLC*. [http://dx.doi.org/10.1063/1.4901966]

I. INTRODUCTION

Broadband sensors are a key element in many ultrasonic systems for applications such as imaging and materials characterization. The design of broadband sensors differs significantly from that of resonant devices since it requires the modeling of wave propagation in the sensor material, including explicitly its interaction with the surrounding media. It is also necessary to take into account the dependence of materials properties on frequency and, in many applications, also on temperature.

The detailed knowledge of the properties and behavior of piezoelectric polymers is a requisite for an efficient implementation of sensors and systems based on these materials. In particular, the effect of dielectric and mechanical relaxation processes has a strong impact on the performance of polymer-based sensors. From the design perspective, it is advantageous to have a comprehensive model to predict the performance of a sensor considering all the previously indicated aspects. A number of papers have been published in this context, but the majority of the models are only applicable within a narrow frequency range, close to the mechanical resonances of the devices.[1–5] Therefore, the usefulness of those models as design tools for broadband sensors is limited.

Poly(vinylidene flouride) (PVDF) and its copolymers are, at present, of great interest since are flexible, available as thin films and have large acoustic bandwidth. Moreover, their acoustic impedance, within the frequency range of interest, is close to that of water or living tissue.[6] These properties make them useful for biomedical applications, since their advantages outweigh the larger dielectric and mechanical losses, as well as the relatively low piezoelectric coefficient of these materials.

This paper presents a model suitable to design and characterize broadband thin film sensors based on piezoelectric polymers. The treatment aims at a balance between complexity and completeness, thus describing adequately the sensor behavior, with a reasonable number of parameters and based on well-known physical equations. The electromechanical variables are described by an acoustic transmission line. The line parameters were calculated from measured values of the material properties (including losses and piezoelectric effects) in the frequency and temperature ranges of interest. The model was validated with measurements of a PVDF-based sensor for the detection of short pulses generated by a Q-switched laser, such as those found in the characterization of complex fluids by photoacoustic techniques.[7,8]

II. PROPAGATION MODEL IN A PIEZOELECTRIC POLYMER

In the present model, it is assumed that one-dimensional (1-D) pressure waves (forward and backward) propagate in the poling direction of a piezoelectric thin film indicated as the reference axis 3 or z (see Fig. 1). In the quasi-static approximation (considering that the film thickness is much smaller than the wavelength in the material), a piezoelectric film can be treated as a two-port network made of discrete circuit elements. This network relates electrical quantities at one port to mechanical quantities at the other. Close to the mechanical resonances, when the thickness of the film is near a

a)Author to whom correspondence should be addressed. Electronic mail: mggonza@fi.uba.ar

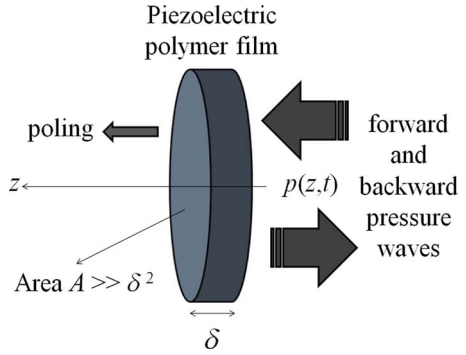

FIG. 1. Geometry of the propagation model.

half wavelength (acoustic) in the polymer, the low frequency lumped model is no longer valid. To extend the range of applicability of the mechanical model beyond the quasi-static approximation, the piezoelectric polymer can be modeled with distributed parameters, as in an electrical transmission line. On the other hand, from the electrical point of view, the quasi-static description is still appropriate given the enormous difference between the velocities of propagation of the electrical and mechanical disturbances.

In the 1-D treatment of a continuous medium by a transmission line model, the variables are constant in the planes perpendicular to the wave propagation direction, but not along it.[9,10] Therefore, the sound pressure and volume velocity field are written as $p(z,t)$ and $u(z,t)$, respectively. In consequence, the transmission line model can be treated using the "telegrapher's equations" in a manner analogous to a lossy electrical transmission line. Then, the line is discretized as a sequence or cascade of two-port network of length dz. Assuming a harmonic time dependence

$$p(z,t) = P(z,\omega)\cdot\exp(j\omega t), \tag{1}$$

$$u(z,t) = U(z,\omega)\cdot\exp(j\omega t). \tag{2}$$

From the well-known analogies between voltage and sound pressure, and electrical current and volume velocity, the equations in the frequency domain are[9,10]

$$\frac{dP(z,\omega)}{dz} + j\cdot\omega\cdot L_z^*(\omega)\cdot U(z,\omega) = 0, \tag{3}$$

$$\frac{dU(z,\omega)}{dz} + j\cdot\omega\cdot C_z^*(\omega)\cdot P(z,\omega) = 0, \tag{4}$$

where j is the imaginary unit, $L_z{}^*$ and $C_z{}^*$ are the complex inductance and capacitance per unit length of the transmission line, respectively. These complex parameters include the dissipative processes, usually modeled as a series resistance and parallel conductance. In what follows, the frequency dependence will be assumed and will not be indicated explicitly.

Given the electromechanical coupling originated by the piezoelectric effect, $C_z{}^*$ must include both the effects of the elastic properties of the material and the mechanical equivalent of the electrical properties. Since we consider a non-magnetic material, $L_z{}^*$ includes only the mechanical properties (see Fig. 2).

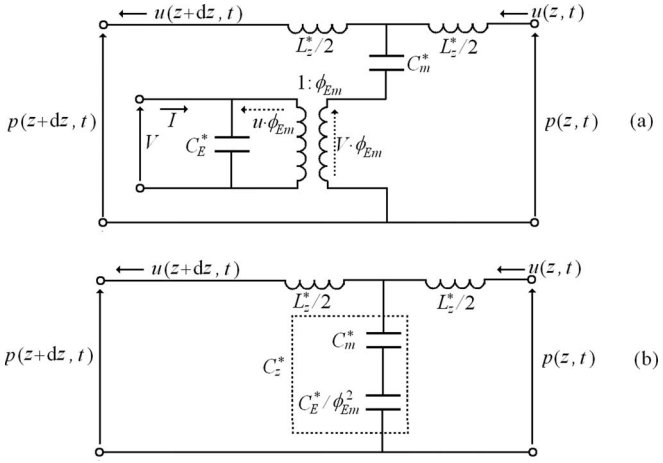

FIG. 2. (a) Unit element of the transmission line. (b) Under quasi-static approximation of the electrical variables. ϕ_{EM} is the turn ratio of the ideal transformer linking electrical to mechanical sides of the network.

The line mechanical parameters can be determined by[9]

$$L_z^* = \frac{\rho}{A}, \tag{5}$$

$$C_z^* = \frac{A}{\rho\cdot v^2}, \tag{6}$$

where v is the complex sound velocity of the material, and ρ and A are the density and area of the film, respectively. The sound velocity can be written in terms of the intensive parameters of the piezoelectric material, assumed to be at constant temperature

$$v = \sqrt{\frac{c_{33}^D}{\rho}}, \tag{7}$$

$$c_{33}^D = \frac{d_{33}^2}{s_{33}^2\cdot\varepsilon_{33}^F} + \frac{1}{s_{33}}, \tag{8}$$

where d_{33} is the piezoelectric coefficient, s_{33} is the elastic compliance at constant electric field, and $\varepsilon^F{}_{33}$ is the complex permittivity at zero stress condition. The complex permittivity at zero strain condition, $\varepsilon_{33}{}^B$, can be related to $\varepsilon_{33}{}^F$ by

$$\varepsilon_{33}^B = \varepsilon_{33}^F - \frac{d_{33}^2}{s_{33}}. \tag{9}$$

It is important to remark that the dependence of the materials properties on temperature, T, is not explicitly written in the previous equations, but it must be taken into account in the modeling.

In this work, we suppose that the polarization instantaneously follows the mechanical deformation. This can be justified by noting that the total piezoelectric effect due to deformation can be written as a sum of two terms of different origins: (i) volume change and (ii) reorientation of the elementary dipoles of the crystalline phase. Although we cannot exclude *a priori* the existence of a delay between deformation and dipole reorientation in the crystalline phase, according to the work of Broadhurst *et al.*[11] the effect of volume change is clearly predominant in the PVDF, as is the case in most piezoelectric polymers. Hence, there is no serious error if the reorientation delay is neglected. Therefore, from (9) it follows

that the difference between the free and blocked permittivities is proportional to the elastic compliance, i.e., d_{33} is proportional to s_{33},

$$d_{33} = \sigma_{33} \cdot s_{33}, \tag{10}$$

where σ_{33} is the equivalent surface charge density of remnant polarization and under this model is a real number, within the relevant frequency range.

Using (9), (10), (6), and (8) can be rewritten as follows:

$$c_{33}^{D} = \sigma_{33}^{2} \cdot \left[\frac{1}{\varepsilon_{33}^{F} - \varepsilon_{33}^{B}} + \frac{1}{\varepsilon_{33}^{F}}\right], \tag{11}$$

$$C_{z}^{*} = \frac{A}{\sigma_{33}^{2} \cdot \left[\frac{1}{\varepsilon_{33}^{F} - \varepsilon_{33}^{B}} + \frac{1}{\varepsilon_{33}^{F}}\right]}. \tag{12}$$

Using (12) the complex equivalent capacitance can be calculated from measurable parameters. It must be kept in mind that the parameters of the electrical and mechanical spectra depend on temperature.

Given that the electrical variables are treated used the quasi-static approximation, the instantaneous charge generated on the surface of the film is calculated as proportional to the integral of the pressure along the z axis (direction of propagation and poling direction),

$$q_P(t) \propto \int_0^{\delta} p(z,t) \cdot dz, \tag{13}$$

where δ is the thickness of the film. It must be remarked that the output current of the sensor is given by $\mathrm{d}q_p(t)/\mathrm{d}t$.

III. EXPERIMENTAL

A sensor made of a thin film piezoelectric polymer, encapsulated in a standard BNC connector was implemented, following the design in Schmid *et al.*[12] This sensor was attached to a spectroscopy-quality quartz cuvette. It is important to note that this design has been used successfully to characterize complex liquid samples.[7,8,13] The complete experimental setup is shown in Fig. 3. A Nd:YAG laser with a second harmonic generator (Continuum Minilite I, 520 nm, 5 ns, 10 Hz) was used to generate a pressure signal on the silver paint layer that adheres the piezoelectric film to the cuvette. To amplify the signal generated by the sensor, a transimpedance amplifier (Femto HCA-100M-50K-C) was used. The amplifier output was digitized by an oscilloscope (Tektronix TDS 2024, 2 GS/s, 200 MHz) and processed on a personal computer. The oscilloscope trigger signal was obtained from the Q-switch pulse.

A sample of the main laser beam was taken by a beamsplitter to measure the laser pulse energy with a pyroelectric detector (Coherent LMP10). Also, a diverging lens was used to uniformly illuminate the surface of the sensor. The cuvette was filled with deionized water; and its temperature was monitored using a calibrated thermocouple. In this way, the sensor can be characterized under realistic operating conditions, at different temperatures.

It is important to remark that the frequency response of the amplifier was determined independently using a network analyzer at frequencies up to 200 MHz. In this way, its effect on the digitalized signal was considered. The frequency response fits very well to a second order transfer with constants $K = 49.2$ kV/A, $\omega_0 = 628.3$ M/s, and $Q_0 = 0.34$,

$$T_A(j \cdot \omega) = \frac{K \cdot \omega_0^2}{\omega^2 + j \cdot \omega \cdot \omega_0/Q_0 + \omega_0^2}. \tag{14}$$

The sensor was implemented using PVDF (PIEZOTECH CORP) with a thickness of 25 μm, metalized on both sides, cut as a disk 6 mm in diameter. As it was indicated in a previous work,[14] the electric response of PVDF can be described by a Havriliak-Negami function.[15] At frequencies above 1 MHz, the permittivity is dominated by a relaxation process whose characteristic time presents an exponential dependency with temperature (Arrhenius).[16]

IV. NUMERICAL IMPLEMENTATION

Fig. 4 shows the simplified model of the device described in Sec. III. The transducer is represented by three layers: (1) quartz, (2) silver paint, and (3) PVDF film. The initial time condition is defined by a Gaussian pressure pulse in layer 2 (silver paint), following the measured laser time profile:

$$p_{in}(t) = p_0 \cdot \exp\left(-t^2/0.36 \cdot \tau_F^2\right), \tag{15}$$

where τ_F is the measured full width at half maximum. For the laser used in this work, $\tau_F \approx 5$ ns.

The transition between the rear face of the PVDF and air is considered as a total reflection, given the huge difference between their respective acoustic impedances. Therefore, the

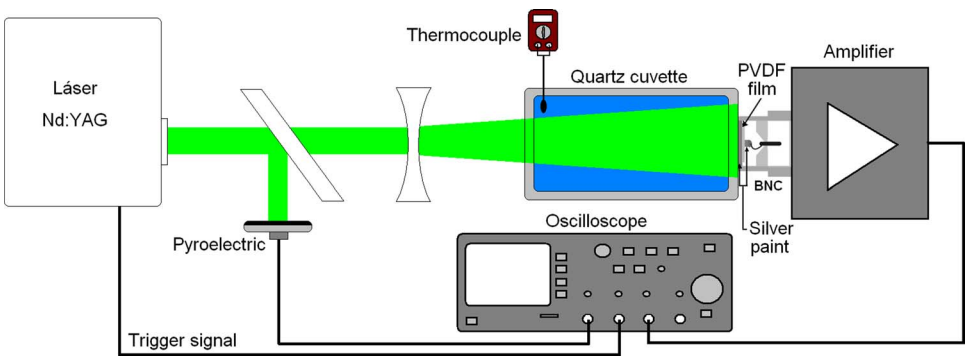

FIG. 3. Experimental setup.

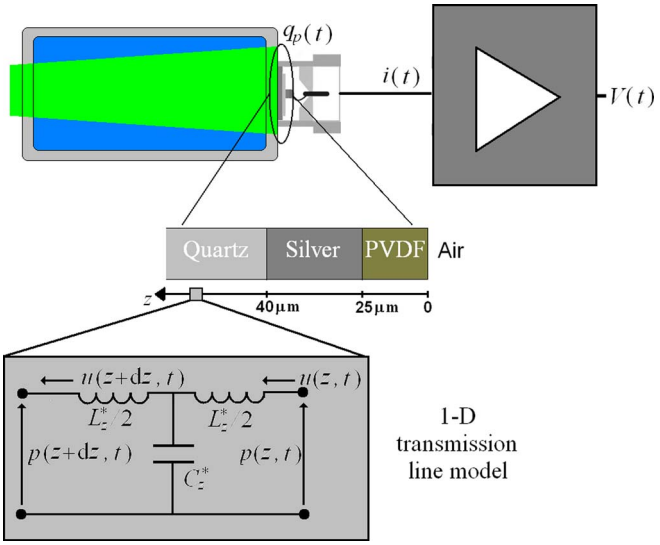

FIG. 4. Scheme of the numerical implementation of the propagation model in a piezoelectric transducer.

boundary conditions are zero both for the pressure (Dirichlet condition) and the volume velocity (Neumann condition). Since the thickness of the quartz is very large compared to the spatial extent of the travelling pulse, the quartz layer can be considered as a semi-infinite medium at all the frequencies of interest. In fact, the backward pulse reflected from quartz-water interface can be neglected because it is delayed out of the time frame of the analysis.

It is considered that the mechanical properties of layers 1 ($\rho_1 = 2200$ kg/m^3, $v_1 = 5900$ m/s) and 2 ($\rho_2 = 6500$ kg/m^3, $v_2 = 2550$ m/s) do not depend on the frequency and they are substantially constant within the temperature range studied in this work. Also, the values of ρ_3 y σ_{33} used in the model were taken as constants, 1780 kg/m^3 and 7.7 μC/cm^2,[17] respectively. In consequence, L_z^* is a constant independent of the frequency.

The transmission line parameters are determined, in the frequency domain, from the dielectric spectra in the free (zero stress) and blocked (zero strain) conditions using (12). However, the measured sensor response to a pulsed excitation is obtained in the time domain. Therefore, the general solution involves transforming the input signal to the sensor, $p_{in}(t)$, to the frequency domain, solving the propagation in the transmission line and then, anti-transforming to have the response in the time domain. This can be a computationally expensive task.

In this work, we propose a computationally simpler solution in which the line parameters used in the simulation are averaged values in the frequency band $\Delta\omega$ where the pulse has appreciable energy. This is an adequate approximation for applications that involve pulses of width $\sim 1/\Delta\omega$. Therefore, the effective complex capacitance $\tilde{C}_z$ is calculated from the averaged complex permittivities $\langle \varepsilon_{33}{}^{\tilde{F}}(T) \rangle$ and $\langle \varepsilon_{33}{}^{B}(T) \rangle$,

$$\langle \varepsilon_{33^{F,B}}(T) \rangle = \frac{\int_0^{\Delta\omega} \varepsilon_{33^{F,B}}(\omega, T) \cdot |P_{in}(\omega)| \cdot d\omega}{\int_0^{\Delta\omega} |P_{in}(\omega)| \cdot d\omega}. \quad (16)$$

Once $\tilde{C}_z$ is determined at a given temperature, the spatial evolution is solved numerically by the finite element method. Furthermore, for time evolution, the Crank-Nicholson finite difference scheme was used. The current at the input of the transimpedance amplifier $i(t)$ is obtained as the time derivative of the charge $q_p(t)$, determined from (13). The output voltage $V(t)$ is calculated as a function of time taking into account the frequency response of the amplifier, Eq. (14).

The numerical simulations were carried out with a program developed in the OCTAVE environment. The parameters adopted in the finite element method were 1001 nodes with a uniform mesh, giving a spatial resolution of 0.5 μm, and time steps of 0.05 ns.

V. RESULTS AND DISCUSSION

Experimental results were obtained at temperatures between 283 K and 313 K. This range was selected for two reasons: (a) it is particular important for applications in biology and medicine, and (b) the lower temperature studied is significantly above the glass transition of PVDF. In connection with this, it must be remarked that the application of this model near the glass transition of the polymer requires further study. On the other hand, the experimental temperature range is wide enough to show clearly the influence of temperature on the sensor response. This is not surprising given the value of the activation energy of the Arrhenius process that controls the dielectric relaxation of PVDF in the frequency range of interest.[14]

An example of the results of the simulation is shown in Fig. 5. The temporal evolutions of the pressure at three z values, as well as the charge on the electrodes, are plotted. It is worth mentioning that the pressure pulse is markedly attenuated due to the electromechanical coupling with the material losses. Therefore, the reflected wave at the back of the sensor is almost negligible. The sign change in the pressure waveform reflects the elastic response of the material.

Since the transit time of the pressure pulse in the film ($\sim\delta/v$) is longer than τ_F, $q_P(t)$ differs from $p_{in}(t)$. This

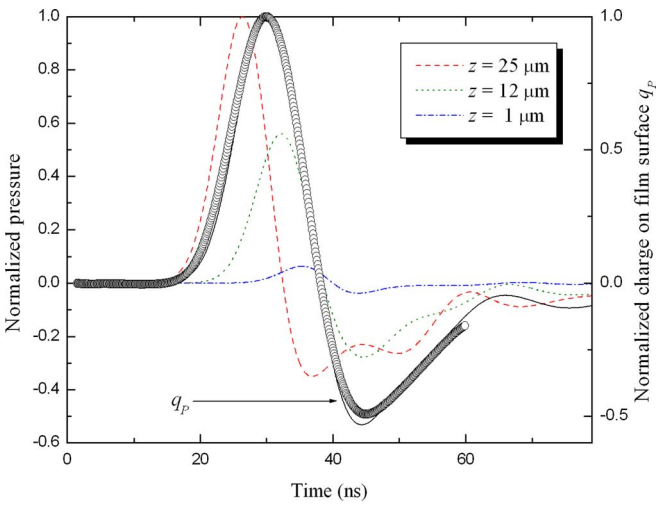

FIG. 5. Normalized pressure at three different positions inside the film (dashed curves). Normalized charge q_P: measured (open circles) and simulated (solid curve). $T = 304$ K.

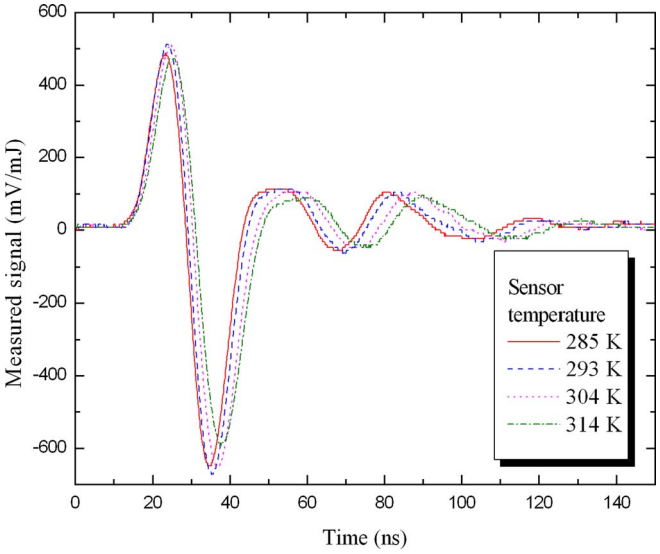

FIG. 6. Signals measured by the sensor at four temperatures.

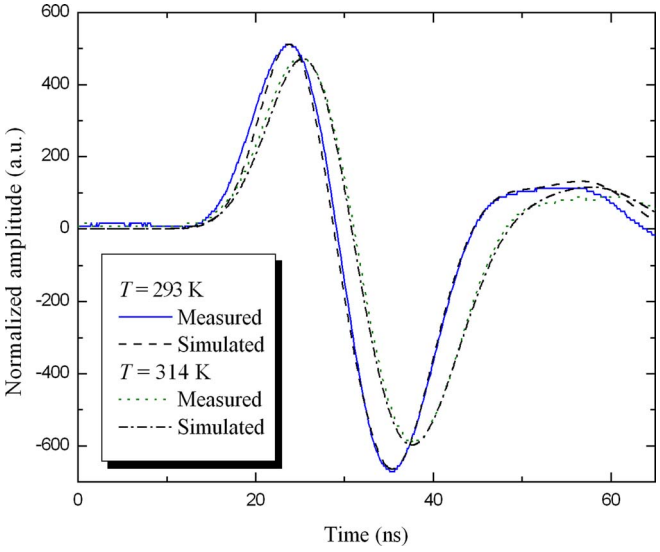

FIG. 8. Comparison between measured and simulated transducer signal.

emphasizes the fact that the mechanical variables must be calculated from a distributed model.

The output signals of the amplifier for the setup of Fig. 3 at different temperatures are plotted in Fig. 6. The plots clearly show the effects of temperature on the sensor performance. As indicated above, this was expected, given the change of PVDF properties with temperature. In particular, the Arrhenius dependence of the relaxation time[14] originates a noticeable modification of the time-domain response. This is a feature often overlooked in previous published models of PVDF transducers.[1–5]

In the first set of numerical simulations, the dielectric spectra of PVDF reported in Ref. 14 were used in (12) and (16) to calculate the effective complex capacitance $\tilde{C}_z$ at different temperatures. Figs. 7 and 8 show the experimental data and the simulations results for the first 65 ns after the excitation pulse. The simulations agree closely with the measured signals; confirming that it is possible to predict the behavior of the sensor directly from the dielectric spectra of the piezoelectric polymer. The simulations describe well the effects of the acoustic reflections at the interfaces and the attenuation originated by the losses in PVDF.

From the digitized amplifier output and its electrical transfer function it is possible to compute $q_P(t)$ (see Fig. 5).

To validate the model, a second set of simulation was carried out assuming that the dielectric spectra ${\varepsilon_{33}}^F$ and ${\varepsilon_{33}}^B$ were unknown. Therefore, $\tilde{C}_z$ was taken as a free parameter, in order to fit the observed signals. The results of both sets of simulations are plotted in Fig. 9. The graph shows the imaginary part of $\tilde{C}_z$ (that represents the average losses of the material) as a function of temperature, normalized to the value at 303 K. The good agreement between the fitting and the calculations shows that it is possible to fit the parameters of the model from the response to a known excitation.

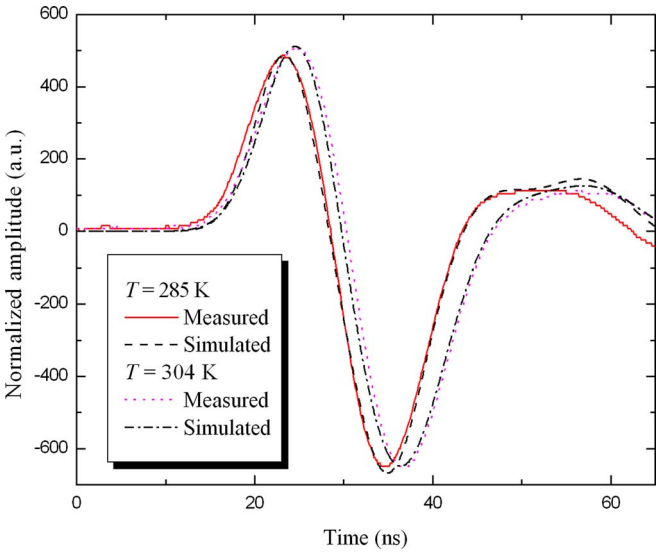

FIG. 7. Comparison between measured and simulated transducer signal.

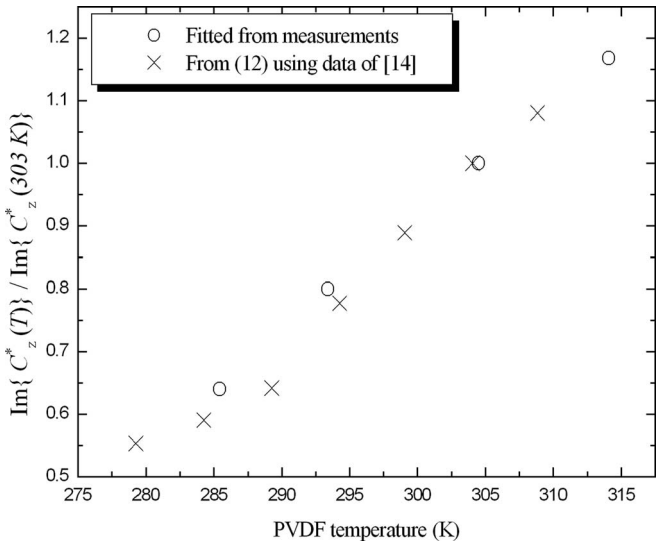

FIG. 9. Normalized imaginary part of the averaged complex capacitance as a function of transducer temperature. $\mathrm{Im}\{\tilde{C}_z(303\ \mathrm{K})\} = 27.5\ \mu\mathrm{m}^4/\mathrm{N}$.

VI. CONCLUSIONS

This work presents a model of sensors based on thin film piezoelectric polymers, adequate for design, and characterization properties. Acoustic propagation is described by an equivalent transmission line model. The dependence of the electrical and mechanical material properties on frequency and temperature is explicitly included.

The model was validated at different temperatures, by measurements in a PVDF-based sensor for short-pulse detection. The results agree very well with the experimental data, predicting satisfactorily the influence of temperature and acoustic impedance mismatches on the transducer performance. Moreover, by taking into account the losses in the polymer, it is possible to optimize the design, minimizing the effects of acoustic reflections.

In conclusion, the model predicts accurately the behavior of the sensor from the material properties. Conversely, by fitting the parameters of the model to the response to a known excitation, the properties of the polymer can be obtained. This is useful when the sensor material has not been fully characterized.

ACKNOWLEDGMENTS

This work was supported by the University of Buenos Aires, Grant Nos. UBACYT-20020100100139; UBACYT-20020120100025; and UBACYT-20020100100406; Consejo Nacional de Investigaciones Científicas y Técnicas (CONICET), Grant No. PIP-112-201101-00676; and the Agencia Nacional de Promoción Científica y Tecnológica, Grant No. PICT-2011-01211.

[1]K. W. Kwok, H. L. Wah Chan, and C. L. Choy, "Evaluation of the material parameters of piezoelectric materials by various methods," IEEE Trans. Ultrason., Ferroelect., Freq. Contr. **44**, 733 (1997).
[2]R. S. Dahiya, M. Valle, and L. Lorenzelli, "SPICE model for lossy piezoelectric polymers," IEEE Trans. Ultrason., Ferroelect., Freq. Contr. **56**, 387 (2009).
[3]IEEE Std. 176-1978, *IEEE Standard on Piezoelectricity* (The Institute of Electrical and Electronics Engineers, New York, 1978).
[4]J. G. Smits, "Iterative method for accurate determination of the real and imaginary parts of the materials coefficients of piezoelectric ceramics," IEEE Trans. Sonics Ultrason. **SU-23**, 393 (1976).
[5]S. Sherrit, H. D. Wiederick, and B. K. Mukherjee, "Non-iterative evaluation of the real and imaginary material constants of piezoelectric resonators," Ferroelectrics **134**, 111 (1992)
[6]L. F. Brown, "Design considerations for piezoelectric polymer ultrasound transducers," IEEE Trans. Ultrason., Ferroelect., Freq. Contr. **47**, 1377 (2000).
[7]T. Schmid, U. Panne, R. Niessner, and C. Haisch, "Optical absorbance measurements of opaque liquids by pulsed laser photoacoustic spectroscopy," Anal. Chem. **81**, 2403 (2009).
[8]M. G. González, X. Liu, R. Niessner, and C. Haisch, "Lead ion detection in turbid media by pulsed photoacoustic spectrometry based on dissolution of gold nanoparticles," Sens. Actuat. B-Chem. **150**, 770 (2010).
[9]L. L. Beranek, *Acoustics* (Acoustical Society of America, New York, 1954).
[10]L. E. Kinsler, A. R. Frey, A. B. Coppens, and J. V. Sanders, *Fundamentals of Acoustics* (John Wiley & Sons, New York, 2000).
[11]M. G. Broadhurst, G. T. Davis, J. E. McKinney, and R. E. Collins, "Piezoelectricity and pyroelectricity in polyvinylidene fluoride—A model," J. Appl. Phys. **49**, 4992 (1978).
[12]T. Schmid, C. Helmbrecht, C. Haisch, U. Panne, and R. Niessner, "Online monitoring of opaque liquids by photoacoustic spectroscopy," Anal. Bioanal. Chem. **375**, 1130 (2003).
[13]X. Liu, M. G. González, R. Niessner, and C. Haisch, "Strong size-dependent photoacoustic effect on gold nanoparticles: A sensitive tool for aggregation-based colorimetric protein detection," Anal. Methods **4**, 309 (2012).
[14]L. Ciocci Brazzano, P. A. Sorichetti, G. D. Santiago, and M. G. González, "Broadband dielectric characterization of piezoelectric poly(vinylidene flouride)thin films between 278 K and 308 K," Polym. Test. **32**, 1186 (2013).
[15]S. Havriliak and S. Negami, "A complex plane analysis of α-dispersions in some polymer systems," J. Polym. Sci., Polym. Symp. **14**, 99 (1966).
[16]J. P. Runt and J. J. Fitzgerald, *Dielectric Spectroscopy of Polymeric Materials: Fundamentals and Applications* (American Chemical Society, Washington, DC, 1997).
[17]M. G. González, P. A. Sorichetti, L. Ciocci Brazzano, and G. D. Santiago, "Electromechanical characterization of piezoelectric polymer thin films in a broad frequency range," Polym. Test. **37**, 163 (2014).